Research Square

Preprints are preliminary reports that have not undergone peer review.
They should not be considered conclusive, used to inform clinical practice,
or referenced by the media as validated information.

A Novel Fluorescent Probe for the Detection of Cyanide Ions in Solutions and Studies on Its Biophysical Interactions with ctDNA and Proteases

Bensu Doyuran
Hacettepe University
Elmas Gökoğlu (gokoglu@hacettepe.edu.tr)
Hacettepe University
Ayman Zouitini
Gazi University
Ergin Keleş
Gazi University
Tugba Taskin-Tok
Gaziantep University
Nurgül Seferoğlu
Gazi University
Zeynel Seferoğlu
Gazi University

Research Article

Keywords: Styrylindolium dye , CN- ions , Pepsin , Trypsin , FRET

Posted Date: July 15th, 2022

DOI: https://doi.org/10.21203/rs.3.rs-1815354/v1

License: This work is licensed under a Creative Commons Attribution 4.0 International License.
Read Full License

A Novel Fluorescent Probe for the Detection of Cyanide Ions in Solutions and Studies on Its Biophysical Interactions with ctDNA and Proteases

Bensu Doyuran[1] . Elmas Gökoğlu[1,*] . Ayman Zouitini[2] . Ergin Keleş[2,3] . Tugba Taskin-Tok[4,5] . Nurgül Seferoğlu[3,6]. Zeynel Seferoğlu[2,3]

[1] Department of Chemistry, Hacettepe University, 06800, Ankara, Turkey
[2] Department of Chemistry, Gazi University, 06560, Ankara, Turkey
[3] Technological Dyes and Materials Application and Research Center (TEBAM), Gazi University, 06560, Ankara, Turkey
[4] Department of Chemistry, Gaziantep University, 27310, Gaziantep, Turkey
[5] Department of Bioinformatics and Computational Biology, Gaziantep University, 27310, Gaziantep, Turkey
[6] Department of Advanced Technology, Gazi University, 06560, Ankara, Turkey

*__Corresponding Author:__ Elmas Gökoğlu, E-Mail: gokoglu@hacettepe.edu.tr

Abstract

A new cationic indolium based styryl dye as a fluorescent probe, (*E*)-2-(4-(dibutylamino)styryl)-1,3,3-trimethyl-3*H*-indol-1-ium iodide (**Ci**), was synthesized and its anions selectivity/sensitivity properties /molecular interactions with protease enzymes (pepsin/trypsin) and ctDNA has been studied by spectroscopic and computational methods. The fluorescence measurements at different temperatures indicated that quenching mechanism of enzymes by **Ci** was static. ΔH and ΔS data pointed out electrostatic/hydrophobic interactions with pepsin, and also hydrogen bonds/van der Waals forces with trypsin of **Ci**. According to Förster's non-radiative energy transfer, binding distances (r) were calculated as 3.53/3.27 nm for pepsin/trypsin. It was also investigated that groove binding is effective in interaction with ctDNA. The results were supported with molecular docking analyzes which have same tendency. **Ci** has been demonstrated hypsochromic effect with a decrease in solvent polarity and it showed highly selective colorimetric and fluorometric sensing behavior for cyanide ions in organic solvent and aqueous solution. ^{1}H NMR titration was performed to examine the interaction mechanism between **Ci** and cyanide ions. The LOD values of cyanide ion were reported as 4.87×10^{-9} M and 9.70×10^{-7} M in DMSO and DMSO/H_2O binary mixture, respectively. In addition, sensitivity of **Ci** as a chemosensor to cyanide ions was investigated in bitter almond samples.

Keywords Styrylindolium dye . CN^- ions . Pepsin . Trypsin . FRET

Introduction

Styrylindolium based dyes constitute an important class of merocyanine, they are extensively used in the elaboration of probes for analytes sensing and cell-imaging [1,2]. Besides, styrylindolium cations possess an extended π-conjugation within the indole ring and exhibit visible absorbance and fluorescence emission, and also their central conjugated iminium ion is considered as a good accepting electrophile [3]. The nucleophilic attack on the carbon-nitrogen double bond of the indole (imine) could modify the

photophysical properties, for that reason, styrylindolium based molecules may serve in producing suitable colorimetric and fluorimetric receptors for nucleophilic analytes such as cyanide anions. Thus, the styrylindolium scaffold has been used as a building block for the synthesis of numerous sensors of biologically and environmentally important nucleophiles such as cyanide [4,5], fluoride [6], sulfide [7], amino acids [8]. In addition, several styrylindolium based derivatives for cell imaging have been reported [9,10].

Proteases are large and diverse group of hydrolases, classified according to the domain,the structure of the active site of the enzyme, and the specific reaction mechanism. They are structures that hydrolyze peptide bonds between amino acid residue of proteins [11]. They play important roles in physiological and pathological processes such as cell growth, migration, protein catabolism, blood clotting, protein activation, tissue development, tumor growth, cell regulation and signalling [12]. Pepsin, an aspartic protease enzyme, is involved in digestive processes in the mammal's stomach. It hydrolyzes proteins to peptides and amino acids, resulting in a decrease in its enzyme activity, which can cause nutrient absorption and side effects such as vomiting and nausea. It is widely used in various places such as food and drug production [13]. Pepsin has 326 amino acid residues containing five tryptophan (Trp), thirteen tyrosine (Tyr) and thirteen phenylalanine (Phe) in a single polypeptide enzymatic chain. Trypsin, which is produced in the pancreas and hydrolyses proteins, is a serine protease enzyme found in many vertebrates. It has 223 amino acid residues containing four Trp, ten Tyr and six Phe. It is involved in the digestion and deconstruction of protein in food and also some physiological processes such as immunity, reproduction [14]. The development of suitable fluorescent dyes has provided an opportunity to explore the physiological roles of biomolecules and keeping in view the sensing and biological significances of cationic styryl-based dyes which show a good affinity for DNA and a good cytotoxicity againist some cancer cell lines [15]. Here, a new cationic styrylindolium dye as a chemosensor (given as **Ci** or as dye in text) synthesized to determinate cyanide ion in aqueous media. Also its biophysical interaction and binding properties were investigated with ctDNA and pepsin/trypsin by multi spectroscopic and molecular docking methods in following sections.

Experimental

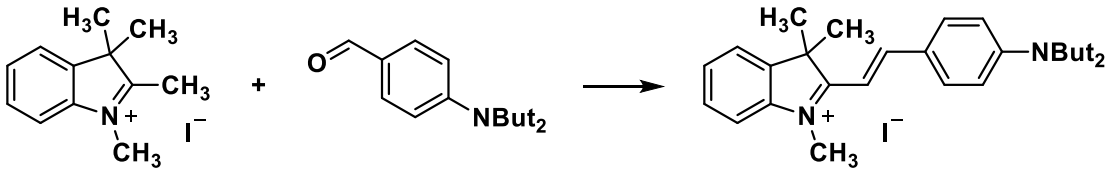
Reagents

Pepsin (EC 3.4.23.1, mol wt: 35 kDa, from porcine gastric mucosa), trypsin (EC 3.4.21.4, mol wt: 23.8 kDa, from bovine pancreas), TBA salts of anions were obtained from Sigma-Aldrich. The solvents were purchased from Alfa Aeser Chemicals and used without further purification. Doubly distilled water was used for preparing buffer solutions and all experimental studies. The stock solution of **Ci** (1.20×10^{-3} M) was prepared in DMSO. The stock solution of trypsin (1.40×10^{-4} M) was prepared in PBS (phosphate buffer solution, 0.067 M) at pH 7.4. The stock solution of pepsin (1.20×10^{-4} M) was prepared in citric acid/citrate buffer solution at pH 2.0. The solutions used in experimental studies were diluted from stock solutions during operation and stored at 4°C.

Synthesis and spectral characterization of Ci

*(E)-2-(4-(dibutylamino)styryl)-1,3,3-trimethyl-3H-indol-1-ium iodide (**Ci**)* which is synthesized following the steps presented in Scheme 1. Compound **1** (1,2,3,3-tetramethyl-3*H*-indol-1-ium iodide) was obtained from the previously reported method [16]. A mixture of compound 1 (1 eq) and 4-(dibutylamino)

benzaldehyde (1 eq) and a catalytic amount of piperidine in 20 mL of ethanol was heated under reflux overnight. the solvent was evaporated after cooling down at room temperature.The column chromatography (MeOH/DCM, 1/5) was used to purify the crude mixture. The pure form of **Ci** was obtained dark green powder. Yield 89%, m.p. 70-72°C.



1 **Ci**

Scheme 1 Synthesis of **Ci**, (*E*)-2-(4-(dibutylamino)styryl)-1,3,3-trimethyl-3*H*-indol-1-ium iodide.

The structural analysis and spectral properties of compound **Ci** were done using FTIR, ^{1}H and ^{13}C NMR, HRMS methods. The related spectra are given in Fig. S1-S4 in Supplementary Information (SI). The synthesis reaction was monitored under UV light on silica gel 60F254 plates (Merck) with thin-layer chromatography (TLC). FTIR spectra were obtained from the Perkin Elmer Spectrum 100 FTIR spectrophotometer. ^{1}H and ^{13}C NMR spectra were recorded on Bruker-Spectrospin Avance Ultra-Shield spectrometer using DMSO-d_6 as sovent and TMS as standard reactive. The electron ionization (EI) mass spectrometry (Waters-LCT-Premier-XE-LTOF (TOF-MS) was used for high resolution mass spectra (HRMS) of compound **Ci**. The melting point data were measured from Electrothermal IA9200 instrument.

^{1}H NMR (300 MHz, DMSO-d_6) δ 8.28 (d, *J* = 15.6 Hz, 1H), 8.03 (d, *J* = 8.6 Hz, 2H), 7.76 (d, *J* = 7.3 Hz, 1H), 7.68 (d, *J* = 7.9 Hz, 1H), 7.54 (t, *J* = 7.6 Hz, 1H), 7.46 (t, *J* = 7.3 Hz, 1H), 7.21 (d, *J* = 15.6 Hz, 1H), 6.85 (d, *J* = 8.8 Hz, 2H), 3.94 (s, 3H), 3.49 (t, *J* = 7.7 Hz, 4H), 1.74 (s, 6H), 1.55 (m, *J* = 7.7 Hz, 4H), 1.36 (m, *J* = 7.3 Hz, 4H), 0.94 (t, *J* = 7.2 Hz, 6H).
^{13}C NMR (400 MHz, DMSO-d_6) δ 179.7, 154.2, 153.3, 142.9, 142.5, 129.1, 127.8, 123.0, 122.4, 113.9, 112.5, 105.1, 51.2, 50.5, 33.5, 29.6, 26.7, 20.0, 14.3.
FTIR (cm^{-1}): 2955 (C-H aliphatic), 1612 (C=N), 1567 (C=C), 1508 (C=C).
HRMS (TOF ES^{+}) (*m/z*), [M+H]$^{+}$ found for $C_{27}H_{37}IN_2$, 389.295 and calcd. for 390.295.

Apparatus and methods

Spectroscopic measurements of dye/enzymes

The fluorescence studies were performed on a Hitachi F-4500 (Japan) spectrofluorometer which contains 150 W xenon lamp and FLSolutions software. The both excitation and emission bandwiths were at 2.5 nm with a scan speed 20 nm/s. The pH values of the study solutions were measured on a Mettler Toledo (FiveEasy Plus) digital pHmeter. The interactions of **Ci**-pepsin/trypsin were studied by the fluorimetric titration method at 298, 303 and 310 K. Intrinsic fluorescence of enzymes was recorded by adding a 5-60 µL volume range of **Ci** stock solution on 2.5x10^{-6} M pepsin and 5.0x10^{-6} M trypsin solutions exciting at 280 nm. The fluorescence titration data were examined to the *Stern-Volmer* quenching model. ΔH and ΔS parameters were calculated from the *van't Hoff* equation. Based on Förster's theory, FRET parameters such as $J(\lambda)$, r, R_0 were obtained between the dye and

enzyme for molecular pairs. For inner filter effect, intrinsic fluorescence of protein was corrected in below equation [17];

$$F_{cor} = F_{obs}\ 10^{(Aex + Aem)/2} \quad (1)$$

A_{ex} and A_{em} are absorbances at wavelengths of excitation and emission; F_{cor} and F_{obs} are corrected and observed fluorescence intensities, respectively.

The FTIR spectra were recorded with a Thermo Scientific Nicolet iS5 which contains iD5 ATR from enzyme solutions ($1.0x10^{-5}$ M) with and without **Ci** compound. Analysis were obtained from a laminate-diamond crystal window at 4 cm^{-1} resolutions with 64 scans in the range of 1700-1500 cm^{-1}.

Far-UV CD spectra were performed from free enzyme ($2.08x10^{-6}$ M) and **Ci**/enzyme complex (1:1 mol ratio) on Jasco-J815 spectropolarimeter (Japan) under constant nitrogen flux using 0.1 cm quartz cell at 298 K. All spectra were taken from 205 to 260 nm wavelength range with scan speed of 50 nm/min and 0.1 nm step resolution. Each result was the average of three replicates.

UV-Vis absorption studies

UV-visible absorption spectra were recorded with a UV-1700PharmaSpec spectrophotometer (Shimadzu) using the UV-Probe PC software program. The UV-vis absorption spectra of **Ci** with and without DNA and pepsin/trypsin were obtained and compared with each other.

Calculation methods

The geometry optimizations of compound Ci were done using Becker's three parameterized Lee-Yang-Par (B3LYP) exchange functional with 6-31+G(d,p) basis set [18]. Density Functional Theory (DFT) method as implemented in the Gaussian 09 package was used for calculations [19]. The electronic absorption spectra were obtained in DMSO using the PCM model using time-dependent DFT (TD-DFT) [20,21]. The molecular docking simulations were performed for **Ci** against pepsin/trypsin and DNA with PDB ID:1PSA, 1AQ7 and 1BNA, respectively. These target models were downloaded from the RCSB protein Data Bank [22] and minimized by using the protocols in Discovery Studio (DS) 3.5 [23]. Molecular electrostatic potential surface (MEPS) maps and frontier molecular orbitals (FMOs) were also generated from the optimized geometry to obtain important insights into the **Ci**. Afterwards, binding sites of the respective targets were defined via sub protocol of DS 3.5 for the docking process. Finally, the prepared **Ci** and target biomolecules have been reacted to the computational visualization technique, molecular docking using Auto Dock 4.2 [24]. Based on docking results, the best modes of **Ci** for each targets were visualized and evaluated of the potential of protein-ligand interactions with help of Discovery Studio (DS) 3.5. The high ranking docked complex for each target was chosen to examine of the binding mode and binding energy value in 200 conformations.

Results and discussion

Photophysical properties of Ci

The solvatochromic behavior of compound **Ci** was examined in five solvents which have different polarities such as toluene, THF, DCM, DMSO and methanol. The results showed that the absorption maximum of **Ci** was blue-shifted with the increase in the polarity of the solvent. As can be seen from Fig.

1, DMSO and methanol with the highest polarity among solvents caused a hypsochromic shift compared to the other three solvents.

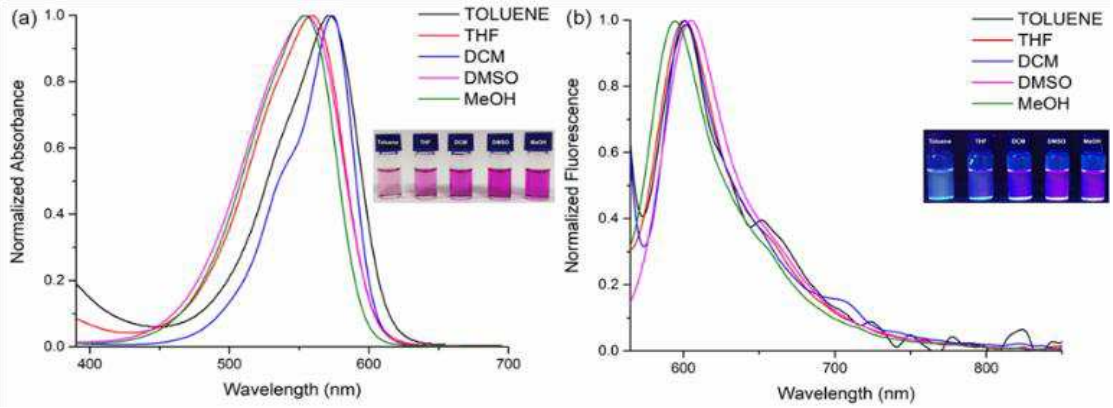


Fig. 1 The normalized (a) absorption and (b) fluorescence spectra of **Ci** ($2x10^{-5}$ M) in five solvents. The photographs of **Ci** (inset) under ambient light (left side) and UV lamp (λ_{ex}=360 nm) (right side) in the solvents.

Anions interactions studies in organic medium

To investigate the detection performance of compound **Ci** as a cyanide ion selective sensor, 1 eq of CN^- and other competing anions such as haloides, AcO^-, ClO_4^-, H_2PO_4, HSO_4^-, NO_3^-, OH^- was added to the DMSO solution of **Ci** to conduct the UV-Vis (c=$2x10^{-5}$ M) and fluorescence (c=$1x10^{-6}$ M) spectroscopic studies. Upon addition of 1 eq of CN^-, the maximum absorption peak of **Ci** showed a significant blue shift from 555 nm to 340 nm (Fig. 2), accompanied with decrease in absorbance. However, for other competing anions, there were no obvious spectral changes.

Besides, for the emission studies, CN^- caused a remarkable change in emission at 607 nm (Fig. 2), while the other competing anions had no apparent effect on the emission spectra. As seen in Fig. 2, the obtained results were confirmed by a dramatic color change after the addition of 1 eq of anions in DMSO. The color of **Ci** changed from purple to colorless in the presence of CN^- observed by naked eyes, while blue emission appeared under the UV light. However, there is no color change for the other anions. These results demonstrate that the synthesized compound could be efficiently used for the selective recognition of cyanide ion through the naked eye in organic medium.

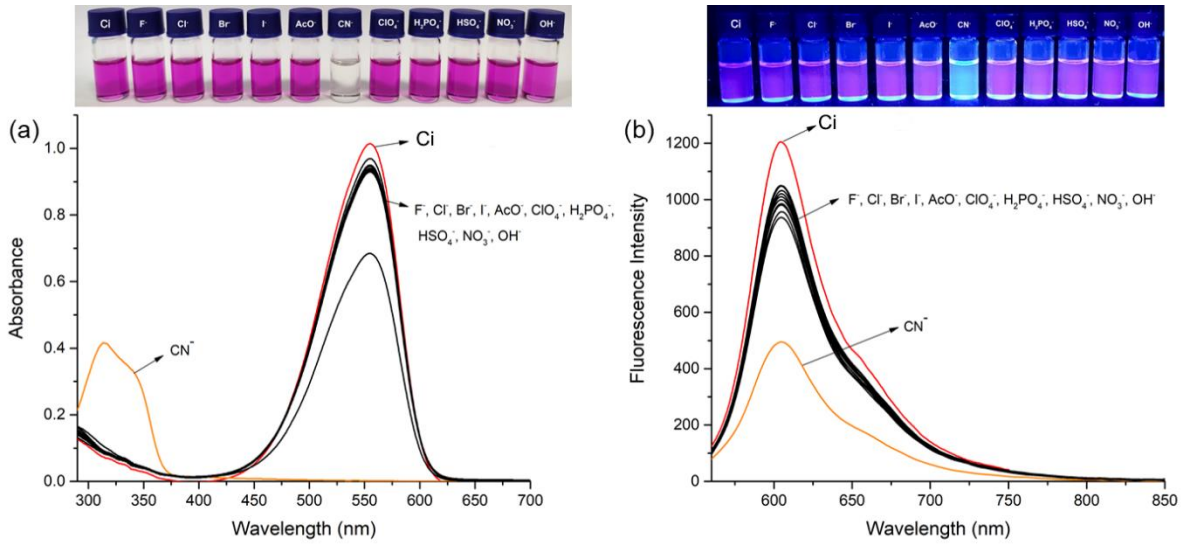


Fig. 2 The absorption (a, c=2.0x10^{-5} M) and fluorescence (b, c=1.0x10^{-6} M) spectra of **Ci** upon the addition of 1 eq of various anions in DMSO. Insets: Photographs color changes after addition of 1 eq amount of anions under ambient light (left side) and UV lamp (λ_{ex}=360 nm) (right side).

To investigate the detection capability of **Ci** towards CN^-, a solution in DMSO of (c =1.0x10^{-6} M) was prepared for fluorescence titration experiments with a range of CN^- concentrations. As shown in Fig. 3, **Ci** (c=1.0x10^{-6} M) has fluorescence property at 607 nm in DMSO. The intensity of the emission decreased by degrees as the concentration of CN^- (0-100 μM) increased. The results suggested that CN^- could cause significant changes in emission performance.

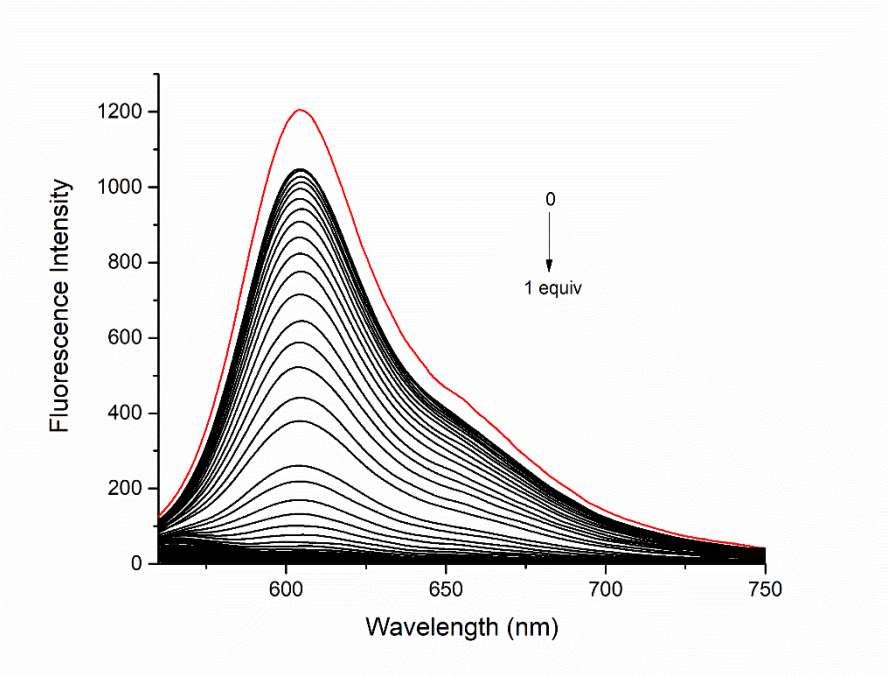


Fig. 3 The fluorescence spectra of **Ci** (1.0x10^{-6} M) in DMSO in the presence of different concentrations of CN^- (0-1 eq).

Anions interactions studies in aqueous medium

Firstly, dye and CN^- interaction was investigated in nine DMSO/H_2O binary solutions ranging from 10/90 to 1/99 (DMSO/H_2O v/v). The UV-vis and fluorescence spectra showed good response in all of the DMSO/H_2O mixtures. As a result, we continued our research in a system containing a binary mixture of DMSO/H_2O (1/99 v/v). By adding increasing concentrations of CN^-, the UV-vis and fluorescence spectra of Ci in an aqueous solution were evaluated. As illustrated in Fig. 4, the band with the highest absorbance at 554 nm diminished, and a new band at 314 nm emerged. Furthermore, the addition of cyanide resulted in a significant decrease in fluorescence intensity.

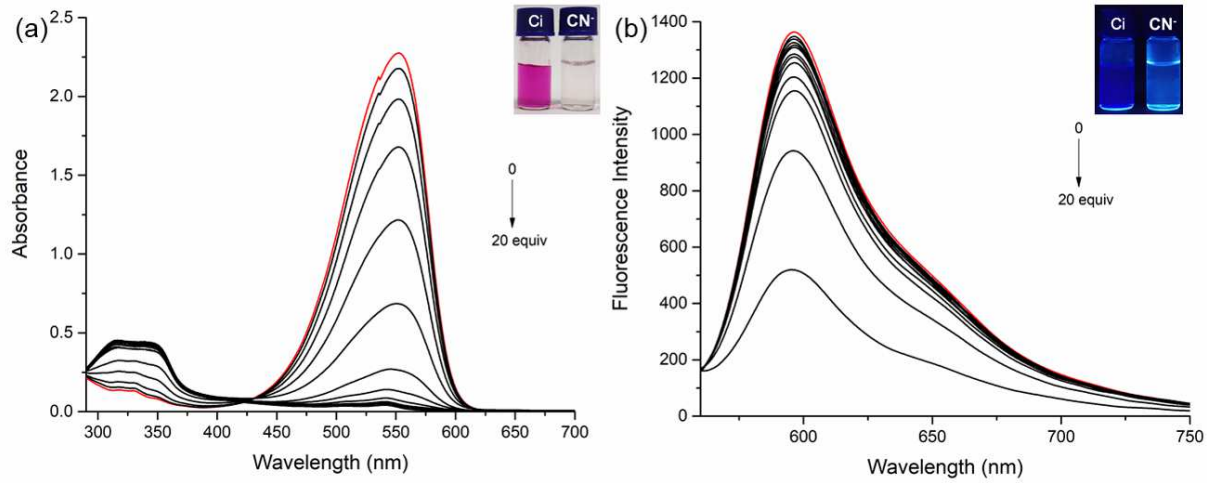


Fig. 4 (a) Absorption and (b) fluorescence spectra of **Ci** ($1x10^{-5}$ M) in DMSO/H_2O (1/99, v/v) in the presence of different concentrations of CN^- (0-20 eq). Insets: Photographs of **Ci** (c=$5.0x10^{-5}$ M) in DMSO/H_2O (1/99, v/v) binary mixture upon the addition of TBACN in daylight and under UV lamp (λ_{ex}=360 nm).

Determination of cyanide ion in real sample

Finally, to investigate the sensor properties, the behavior of **Ci** towards the aqueous solution of bitter almond was examined. For this, the sample of 30 g of crushed bitter almond was placed in flask containg 0.5 g of NaOH and 100 mL of water, after stirring for 20 min final mixture solution was filtered [25]. After the addition of 20 µL of bitter almond, the maximum absorption peak of **Ci** showed a significant blue shift accompanied by a decrease in absorbance. Moreover, a dramatic change in fluorescence intensity was observed at 607 nm in Fig. 5.

The obtained results in UV-vis and fluorescence spectra were confirmed by color change after the addition of 20 µL of bitter almond. The color of **Ci** changed from purple to pale yellow in the presence of CN^- from bitter almond observed by naked eyes, while blue emission appeared under the UV lamp (λ_{ex}=360 nm). These results are in line with those obtained in the CN^- titration study of **Ci** in DMSO. As a result, **Ci** could be applied successfully for the detection of cyanide in bitter almond.

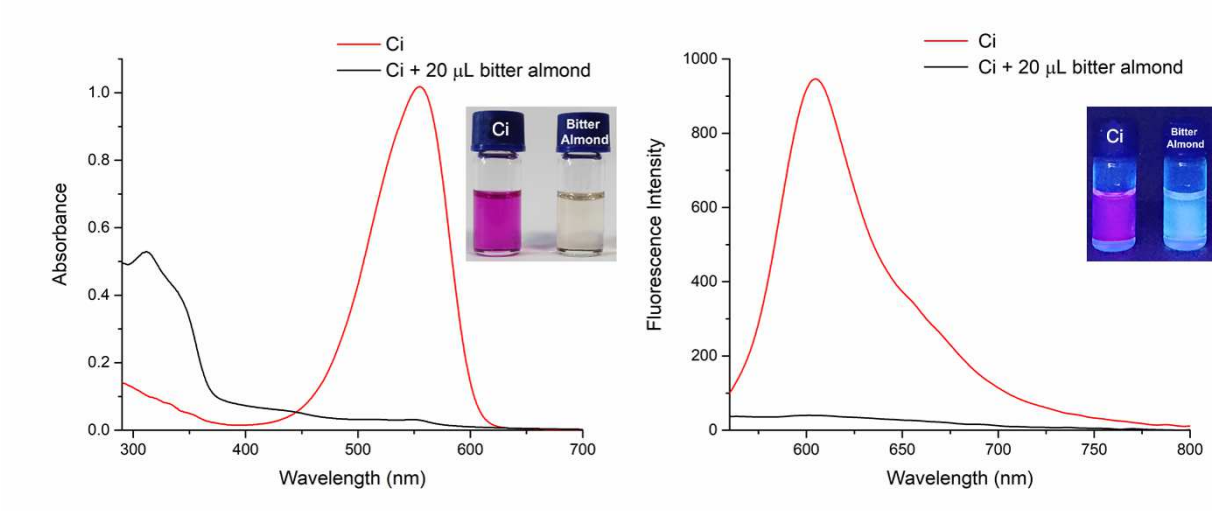


Fig. 5 (a) Absorption and (b) fluorescence spectra of **Ci** (c = 2x10^{-5} M) in DMSO upon the addition of 20 μL bitter almond. Insets: Photographs of **Ci** (c = 5x10^{-5} M) in DMSO upon the addition of 20 μL bitter almond in daylight and under UV lamp (λ_{ex}=360 nm).

Sensing mechanism

In view of the previously reported procedure [26], the sensing mechanism occurring after interaction of cyanide with indole-based molecules is a nucleophilic addition reaction. The cyanide nucleophile attacks the carbon atom of indolium moiety (C=N group) declining its electron-withdrawing ability, hence a change in photophysical properties is observed. To illustrate the sensing mechanism of **Ci**, ^{1}H NMR titration study was explored. ^{1}H NMR titration experiments of **Ci** with different equivalents of cyanide anion (0.5 and 1 eq) were carried out. The ^{1}H NMR spectra were taken for **Ci** and its cyanide adduct using DMSO-d_6 and partial spectra were specified in Fig. 6. As expected, after the addition of 1 eq of cyanide to the **Ci**, the nucleophilic attack of cyanide on the carbon atom of indolium moiety (C=N group) has occurred, and thus the proton signals shifted in high field in the spectrum (Scheme 2). It can be seen that the vinyl protons of **Ci** shifted from 8.29 ppm and 7.3 ppm to 6.7 ppm and 6.05 ppm (Hc and Hd) due to the breaking of conjugation. Besides, the proton signal of a methyl group at 3.95 ppm attached with N$^+$ (He) was shifted up field to 2.69 ppm.

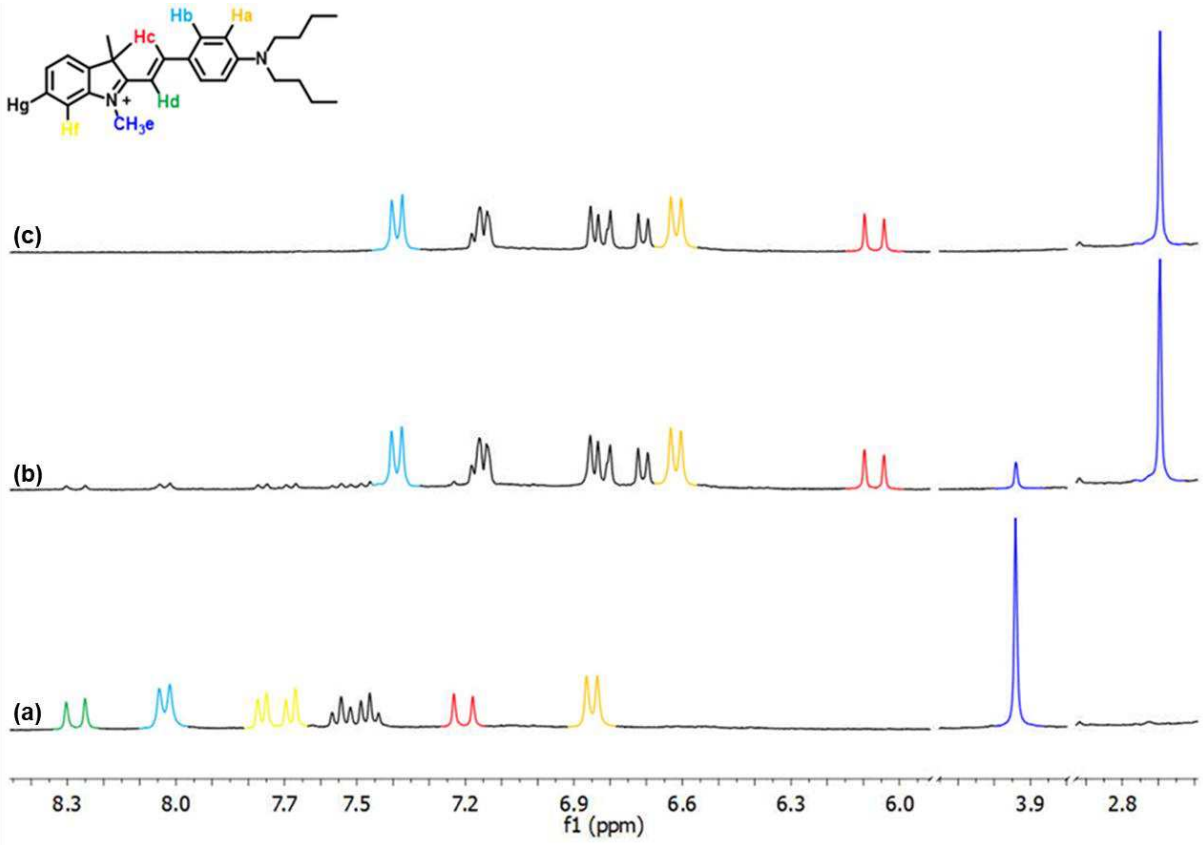
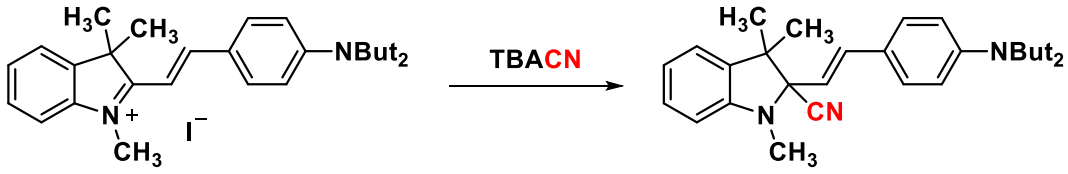


Fig. 6 The ^{1}H NMR titration spectra of **Ci** (a, 10 mM) with 0.5 (b) and 1 (c) eq addition of TBACN in DMSO-d_6.



Scheme 2 The plausible sensing mechanism for the specific determination of CN^-.

To get further information about the interaction of **Ci** with CN^- via addition mechanism, density functional theory (DFT) calculations were performed at B3LYP/6-31+G(d,p) level of theory. As shown in Fig. 7, conjugation between phenyl and indolinium moieties through the styryl bridge disturbed after a nucleophilic attack by the cyanide ion (**Ci** +CN^-). Thus, electron transition from donor group dibutylamino attached phenyl ring to acceptor indolinium moiety is interrupted, resulting in a hypsochromic shifted in absorption spectra. As considering the experimental results, TD-DFT calculations in DMSO showed that the peak at 488 nm (oscillator strength, f=1.7115) seen in absorption spectra of **Ci** shifts to a lower one at 334 nm (f=0.9358). In both cases, the transitions took place as from HOMO to LUMO with the highest contribution (~%99).

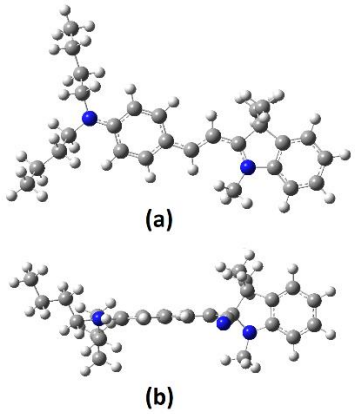


Fig. 7 The optimized geometries of **Ci** (a) and **Ci** + CN^- ion (b).

Quantitative analysis of cyanide ion

The limit of detection (LOD), limit of quantification (LOQ) and the blank sample deviation of cyanide ion in the presence of **Ci** was calculated using the fluorescence titration data obtained above. Table 1 shows these data. The Pearson correlation coefficients of the linear calibration curves were found as 0.9966 in DMSO and 0.9967 in DMSO/H_2O (1/99, v/v) mixture (Fig. S5 in SI). In a dynamic concentration range, the results indicated a good linear relationship between emission intensity and concentration CN^-. According to calculation, the LOD values of **Ci** for cyanide ion were found as $4.9x10^{-9}$ M and $9.7x10^{-7}$ M in DMSO and DMSO/H_2O (1/99, v/v) mixture respectively, which are much lower than the standard limits of CN^- in the aqueous solution set by WHO [27].

Table 1 The LOD and LOQ values of cyanide ion.

Solvent	LOD(M)	LOQ(M)	R^2
DMSO	$4.9x10^{-9}$	$1.6x10^{-8}$	0.9966
DMSO/H_2O*	$9.7x10^{-7}$	$3.2x10^{-6}$	0.9967

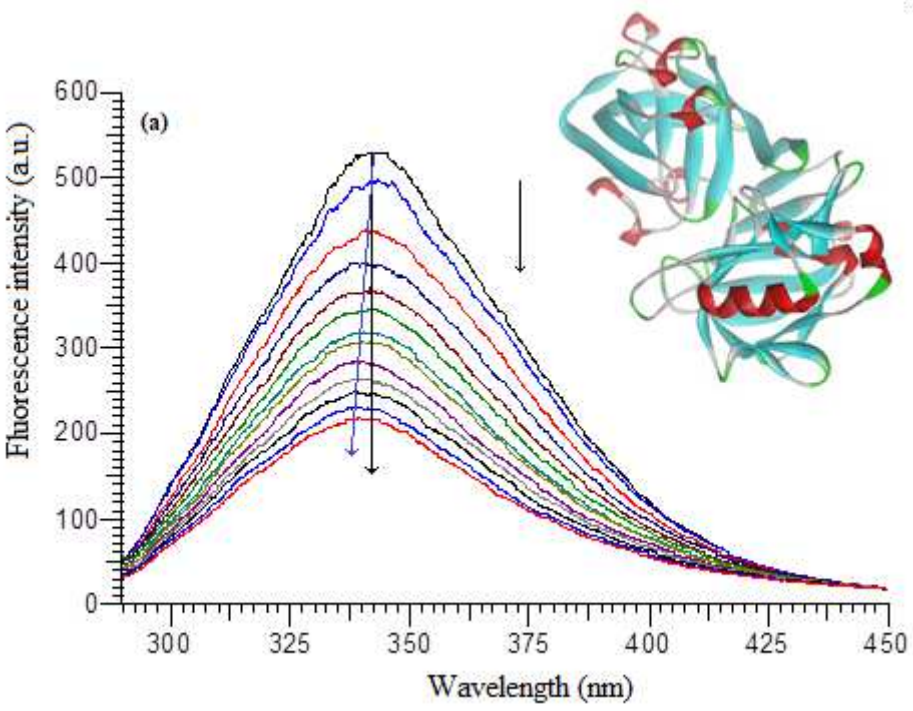
*DMSO/H_2O binary mixture ratio 1/99 (v/v)

Fluorescence quenching of enzymes with Ci

The effects of **Ci** on intrinsic fluorescence from tryptophan residues of pepsin/trypsin are presented with Fig. 8(a) and Fig. 8(b), respectively, at given experimental conditions. The changes in fluorescence intensities in the range 290-450 nm were recorded in the spectra of both enzyme solutions excited at 280 nm. The fluorescence intensities were quenched regularly with a slight blue shift (~5 nm) for pepsin and with a red shift (~10 nm) for trypsin, The fixed concentrations of enzymes were titrated with different amount of **Ci** which added from $2.38x10^{-6}$ M to $2.80x10^{-5}$ M concentration range. This situation can be indicated that it may be due to the non-fluorescent complex formation between **Ci** and pepsin/trypsin. For fluorescent quenching data, the Stern-Volmer equation given below is used [17];

$$F_0 / F = 1 + K_{sv}[Q] = 1 + k_q \tau_0 [Q] \quad (2)$$

where F_0 and F are fluorescence intensities of Trp residues of enzymes in without and with of quencher. K_{sv}, k_q and τ_0 data are Stern-Volmer quenching constant, the quenching rate constant, and average lifetime of biomolecule in the absence of quencher ($\tau_0 = 10^{-8}$) s, respectively. [Q] is concentration of Ci as quencher [28]. The Stern-Volmer graphs were obtained from titration data at 298, 303 and 310 K in Fig. 9(a) for pepsin and Fig. 9(b) for trypsin. Stern-Volmer graphs show good linearity means that the quenching mechanism should be *static* or *dynamic* which can be distinguished by their differing dependence on temperature and excited state lifetime. K_{sv} constants were found the slopes of linear Stern-Volmer graphs and also k_q values were calculated from K_{sv} constants at three temperatures. Based on these data in Table 2, the values of K_{sv} decrease as the temperature increases and it was concluded that the interactions of enzymes with dye are *static* quenching. The maximum diffusion quenching rate constant of diverse biomolecular extinguishers is 2.0×10^{10} L/mol.s and the fact that the k_q values in the table are much larger than this value indicates that there is a *static* quenching mechanism. This indicates the forming of a complex between **Ci** and pepsin/tripsin [29].



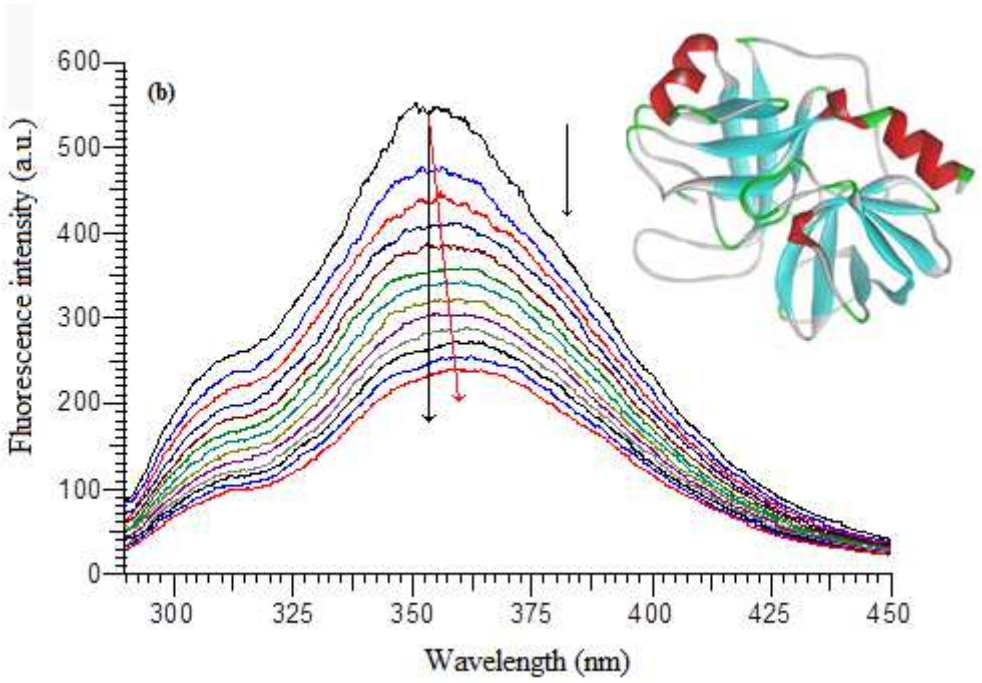


Fig. 8 Effect of **Ci** on the fluorescence spectra of (a) c(*pepsin*)=2.5x10^{-6} M (pH 2.0) and (b) c(*trypsin*)=5.0x10^{-6} M (pH 7.4), λ_{ex}=280 nm, 298 K. c(dye) (from top to bottom): 0, 2.38, 4.75, 7.11, 9.46, 11.8, 14.1, 16.5, 18.8, 21.1, 23.4, 25.7, 28.0 (x10^{-6} M), respectively. The insets show the positions of amino acid residues in the 3D structures of pepsin and trypsin. The green color parts in each target show Trp residues.

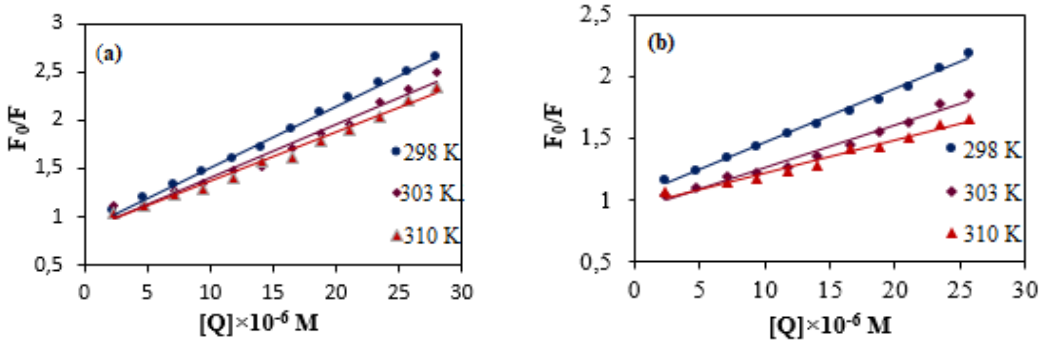


Fig. 9 Stern Volmer graphs for the quenching of pepsin (a) and trypsin (b) by **Ci** at three temperatures. $\lambda_{ex.}$=280 nm; $\lambda_{em.}$ (pepsin) = 343 nm, $\lambda_{em.}$ (trypsin) = 355 nm.

Table 2 The thermodynamic and Stern Volmer parameters of **Ci**-pepsin/trypsin complexes.

	T	K_{sv}	k_q	K	n	ΔH	ΔG	ΔS
	(K)	($x10^4 M^{-1}$)	($x10^{12} M^{-1}s^{-1}$)	($x10^4 M^{-1}$)		(kJ/mol)	(kJ/mol)	(J/molK)
Pepsin	298	6.32	6.32	5.90	1.17	-14.07	-13.11	43.95
	303	5.56	5.56	5.05	1.35		-13.33	
	310	5.11	5.11	4.71	1.36		-13.64	
Trypsin	298	4.33	4.33	4.88	0.82	-36.79	-26.69	-33.87
	303	3.50	3.50	3.60	1.26		-26.53	
	310	2.71	2.71	2.73	1.09		-26.29	

In static quenching interaction, when small molecules bind freely to a set of equal regions on a biomolecule, the equilibrium between free and bound molecules could be identified using fluorescence intensities the following equation [30];

$$\log F_0\text{-}F/F = n\log K - n\log \frac{1}{[Q] - \frac{(F_0\text{-}F)[P]}{F_0}} \qquad (3)$$

where F0, F and [Q] are the same in Eq. 2. K is the binding constant, n is the number of binding sites per protein molecule, and [P] is the total protein concentration. In Fig. 10(a) and Fig.10(b), according to graph of the log $(F_0–F)/F$ vs. $\log(1/([Q]-[P](F_0-F)/F_0))$ at three temperatures for each enzymes, the values of n were obtained from slopes of linear plots and then the values of K were calculated for dye-pepsin/trypsin complexes. The values of n and K are given in Table 2. According to the K values, it can be stated that **Ci** interacts with pepsin with a greater binding constant, that is, **Ci** holds pepsin more firmly than trypsin. The values of n, the stoichiometric binding numbers of the two systems, are approximately equal to 1, which indicates that the **Ci** interacts with one pepsin/trypsin molecule. A decrease in K values occurred with an increase in temperature. This situation, it shows that the stability of complexes decreases with increasing temperature [31].

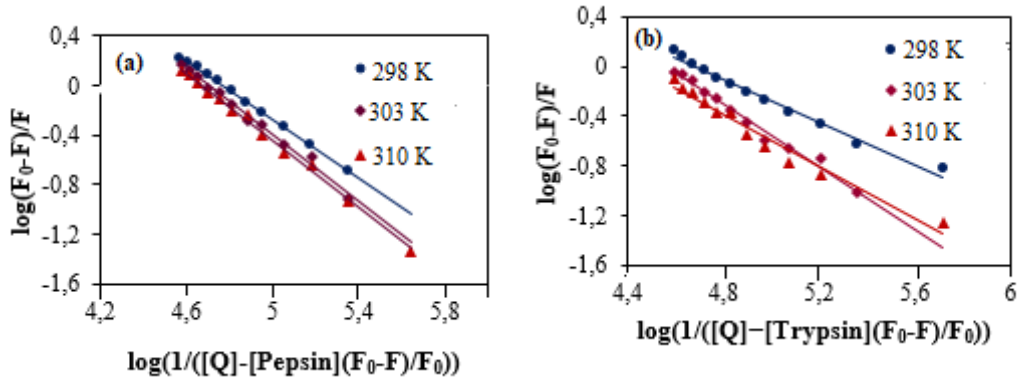


Fig. 10 The graphs of $\log(F_0–F)/F$ vs. $\log(1/([Q]-[P](F_0-F)/F_0))$ for (a) pepsin and (b) trypsin at three temperatures.

Binding modes between Ci and enyzmes

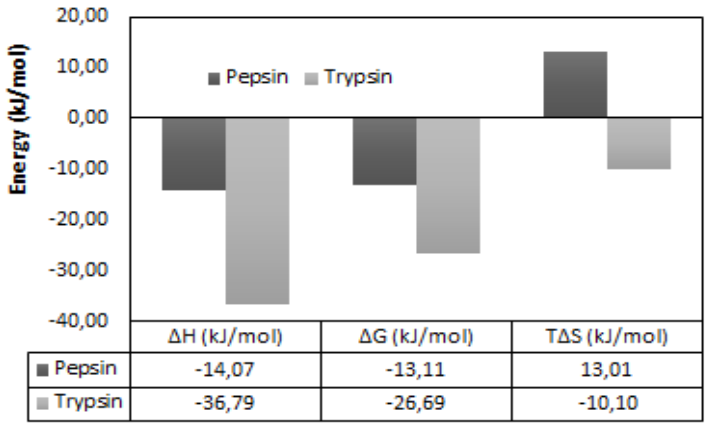
The bonding modes non-covalent interactions between proteins and small molecules are commonly described in terms of hydrophobicity, hydrogen bonds, electrostatic and van der Waals forces. These can be clarified by looking at the magnitude and sign of the thermodynamic parameters of ΔH (enthalpy change) and ΔS (entropy change) [32]. Both the parameters can be determined from the van't Hoff equation;

$$\log K = - \Delta H / 2.303\ RT + \Delta S / 2.303R \quad (4)$$

where K is bonding constant at corresponding temperature and R is the gas constant. Here, the log K values were plotted against 1/T at three temperatures according to Eq. 4. ΔH and ΔS parameters were calculated from the slope and intercept of van't Hoff graphs from their linear equations, log K = 734.72 / 2.303RT + 2.2956 / 2.303R for **Ci** -pepsin and log K = 1921.5 / 2.303 RT -1.7692/ 2.303R for **Ci**-trypsin (Fig. S6 in SI). Then from using Eq. 5, the Gibbs energy change (ΔG) value was calculated in following;

$$\Delta G = \Delta H - T\ \Delta S = - R\ T\ \ln K \quad (5)$$

Table 2 indicates the calculated the thermodynamic parameters of dye-enzyme systems. The histogram graphs of these parameters were given in Fig. 11 at 298 K. Because it appears, negative ΔG indicates that the binding mechanism of **Ci** with enzyme is spontaneous, and the negative ΔH indicates that the binding is exothermic. Positive values for ΔS and negative values for ΔH indicate that electrostatic forces play an active role in Ci-pepsin interactions. However, positive values for ΔS are often considered proof of hydrophobic interaction, since water molecules regularly dispersed round the ligand and protein cause an at random alignment in consequence of the hydrophobic interaction [33]. Within in the interaction between Ci and trypsin, the negative values of ΔS and ΔH indicate that van der Waals forces and hydrogen bonds play significant roles in the bonding mechanism.



	ΔH (kJ/mol)	ΔG (kJ/mol)	TΔS (kJ/mol)
Pepsin	-14,07	-13,11	13,01
Trypsin	-36,79	-26,69	-10,10

Fig. 11 The representation of thermodynamic parameters of pepsin/trypsin interaction with **Ci** at 298 K.

FRET measurements of dye-enzyme pairs

Based on the Förster theory [34], the energy transfer efficiency (E), the critical distance (R_0) at 50% energy transfer and the distance (r) between the donor (pepsin/trypsin) and acceptor (dye) pair were found from experimental results by using equations 6 and 7 in below [17];

$$E = 1 - F / F_0 = R_0^6 / R_0^6 + r^6 \quad (6)$$

$$R_0^6 = 8.79 \times 10^{-25} (\kappa^2 n^{-4} Q_D J(\lambda)) \quad (7)$$

Where n is the refractive index of the medium; k^2 is the orientation factor; and J is called overlap integral. In order to find the J value, the fluorescence spectrum of the enzyme and the absorption spectrum of the dye are found by overlapping. Q_D is the quantum yield of the donor. The spectral overlaps (dye/enzyme= 1:1) were given in Fig. S7 and Fig. S8 in SI at experimental conditions for pepsin and trypsin, respectively. The value of *J* is calculated by the following equation;

$$J(\lambda) = \sum F_D(\lambda) \varepsilon_A(\lambda) \lambda^4 \Delta \lambda \sum F_D(\lambda) \quad (8)$$

where $F_D(\lambda)$ is the normalized donor emission; $\varepsilon_A(\lambda)$ is the molar extinction coefficient of acceptor at given a wavelength. Here, n=1.336 is refractive index of working medium; the fluorescence quantum yields, Q_D are 0.150 for pepsin [35] and 0.146 for trypsin [36]. The E, *J*, R_0 and r results obtained were listed in Table 3. The consequences indicated that the dye-enzyme distance, r, (3.53/3.27 nm) was less than 8 nm, and also the r value was greater than R_0, confirming that non-radiation energy transfer occurred in the static quenching mechanism. Furthermore, the short binding distances indicated **Ci** and tryptophan residues of digestive enzymes produced strong interactions.

Table 3 FRET parameters of **Ci**-pepsin/trypsin.

Donor	Spectral overlap, *J* (L/mol)$cm^3 \times 10^{-14}$	R_0 (nm)	E (%)	r (nm)
Pepsin	1.231	2.64	14.9	3.53
Trypsin	1.090	2.58	19.2	3.27

FTIR studies of dye-enzymes

The basic of the FTIR method is to study the transition between the vibrational level of the basis state molecule due to the absorption of light in the infrared zone and the alter in the secondary structure of the protein after binding to the ligand. Amide bonds induce temporary vibrations in the peptide bands emerging from these infrared spectra [37]. Among the amide bands which are vibration bands, amide I (1600-1700 cm^{-1}) is mainly associated with the stretching band C=O, and amide II (1500-1600 cm^{-1}) is the stretching C-N combined with N-H. As can be seen from Fig. S9(a) and Fig. S9(b), the addition of **Ci** changed the position of the absorption peak of the amide bands of pepsin/trypsin. The peak in the amide I and amid II band shifted from 1651.54 cm^{-1} to 1652.24 cm^{-1} and from 1519.51cm^{-1} to 1524.97cm^{-1} for pepsin; and from 1660.05 cm^{-1} to 1652.74 cm^{-1} and from 1601.90 cm^{-1} to 1594.82 cm^{-1} for trypsin, respectively [38]. Shifts in the bands indicate an alter in the secondary structure of the enzyme after binding process.

Circular dichroism (CD) studies of dye-enzymes

CD is a sensitive spectroscopic technique for monitoring changes in protein structure as it interacts with small molecules. Far UV spectra (260-200 nm) were used to define the secondary structure of the protein. Two negative elliptic bands at 208 nm ($\pi \rightarrow *$) and 222 nm ($n \rightarrow \pi *$) are characteristic of the typical α-helix

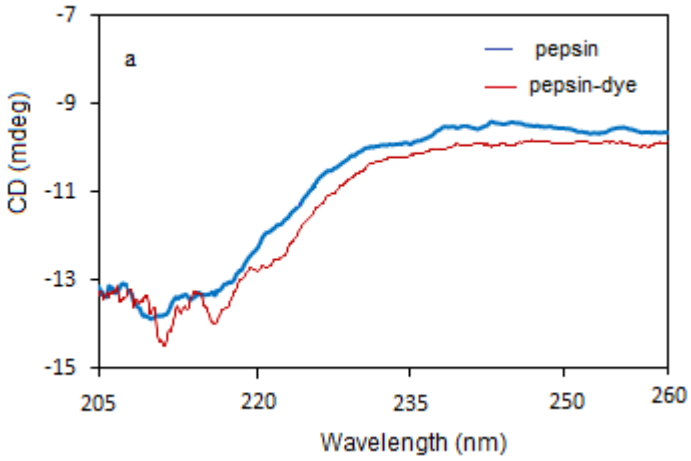
conformation of proteins [39,40]. The CD spectra of pepsin/trypsin in the absence and presence of **Ci** are shown in Fig. 12. CD results were transformed into the mean residual ellipticity (MRE) in deg cm^2/dmol, according to the following equation [41];

$$MRE = \frac{\theta_{obs\ (mdeg)}}{C \times n \times l \times 10} \qquad (9)$$

in equation n, the number of amino acid residues contained in the protein (n, 326 for pepsin and for trypsin 223); C is the molar concentration of protein; θ_{obs} is the observed ellipticity and l is the path length of cuvvette in cm. α-helical contents of free enzyme and dye/enzyme complex was calculated from MRE values at 208 nm using the following equation [42];

$$\alpha\text{-helix}\ (\%) = \frac{-MRE_{208} - 4000}{33{,}000 - 4000} \times 100 \qquad (10)$$

As shown in Fig. 12, the intensity of both bands diminished with the addition of **Ci**, indicating a change in the secondary structure of the enzyme and a diminish in the α-helix content that was shown in Table 4. The results recommended a lessening of α-helical structure percent from 53.55 and 73.90 in free pepsin/trypsin to 52.29 and 70.05 at a molar proportion of chemical to color of 1:1, respectively. As a result, it was clarified that the binding of **Ci** to pepsin/trypsin resulted in a change in the secondary structure of the enzyme with loss of helical stability.



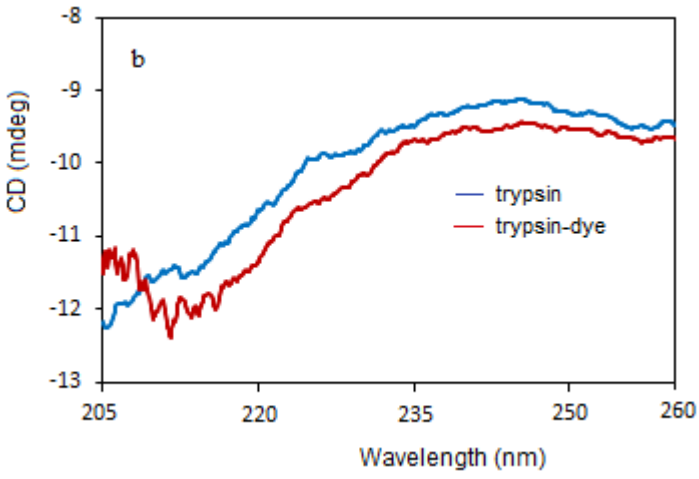


Fig. 12 CD spectra (a and b) of enzyme ($2.08x10^{-6}$ M) in the absence and presence of **Ci** at 1:1ratio of concentration.

Table 4 The α-helix contents of enzymes in the absence and presence of **Ci** at 208 nm.

System	observed CD (mdeg)	α-helix (%)
Free pepsin	-13.26	53.55
Pepsin-dye	-13.01	52.29
Free trypsin	-11.81	73.90
Trypsin-dye	-11.29	70.05

Absorption measurements of dye-enzymes

The UV-visible absorption method is frequently used to examine the complex formation and conformational changes in protein structure that occur in protein-ligand interaction [43]. Absorption spectra of enzymes in the absence and presence of **Ci** were recorded at 298 K in Fig. S10(a) and Fig. S10(b) for pepsin and trypsin, respectively. It can be seen from the spectra with the addition of dye, the maximum peak of absorbance of enzyme at 275 nm which seems to be because of the aromatic amino acid residues increased sharply. The result indicated that there was an alter in the structure of enzyme and the micro environment round the tryptophan residues in dye-enzyme complex.

Binding property of Ci with DNA

The UV-vis absorption is an effective method that shows the changes in absorption and peak position when a complex is formed between DNA and a small molecule, as in proteins. In this case, absorption spectrum of DNA shows hyperchromic and hypochromic impacts associated with its double helix structure. Absorption hyperchromism and blue shift indicate that non-covalent interactions such as electrostatic binding and groove binding damage the secondary structure of the DNA double strand. On the other hand, hypochromism and red absorption shift indicate contraction of DNA in helix axis and structural change of DNA with intercalating binding. [44]. Fig. 13 shows absorption spectra of $1.0x10^{-5}$ M **Ci** *with* and *without* ctDNA were recorded at 298 K and pH 7.4 in PBS. It can be seen the absorption peak at 275 nm of **Ci** displayed gradually increased and a blue shift (~5 nm) the increasing amount (from 0 to $2.97x10^{-5}$ M) of ctDNA. This could be attributed to an interaction between DNA and **Ci** which binds to the DNA helix via groove binding mode.

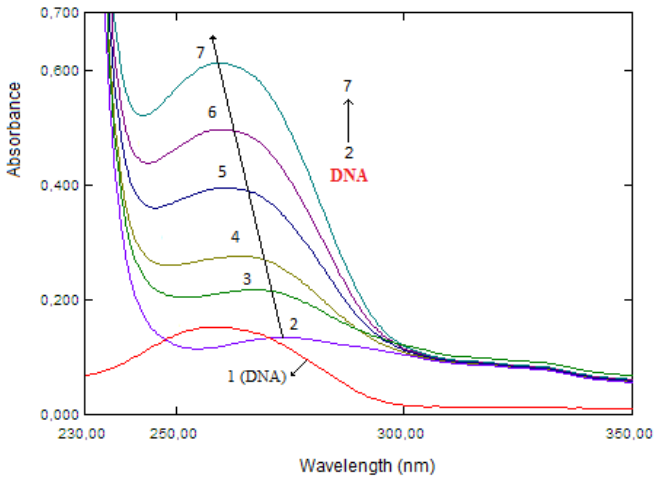


Fig. 13 UV absorption spectra of $1.0x10^{-5}$ M **Ci** (spectrum 2) in the presence of ctDNA. The spectra show (from 2 to 7) addition increasing amount of ctDNA which are 0.0; 6.0; 12.0; 17.9; 23.8; 29.7 ($x10^{-6}$) M. pH 7.4, 298 K. (Spectrum 1 is free $1.0x10^{-5}$ M ctDNA).

Molecular docking results

Optimized **Ci** was performed at G09 on the DFT/B3LYP/6-31+G (d,p) level. To the same level, the frontier molecular orbitals (HOMO and LUMO) and molecular electrostatic potential surface (MEPS) of the respective compound are formed in Fig. 14. The difference in energy between HOMO and LUMO orbital is a measure of electron conductivity. Therefore, it is the parameter used to determine molecular and electrical transport characteristics. Using the energy values of HOMO and LUMO, the chemical potential, electronegativity, electrophilic index, hardness and softness properties of the substance can be calculated [45]. As appeared in figure, the energy difference between HOMO and LUMO is 2.625 eV. The ionization energy using the orbital energies of HOMO and LUMO is $I = -E_{HOMO} = 8.210$ eV and the electron affinity is $A = -E_{LUMO} = 5.585$ eV. Hardness was found to be $\eta=(I- A)/2=1.313$; chemical potential was found to be $\mu=-(I+A)/2=-6.898$; electrophilic index was found to be $\omega=\mu\ 2/2\eta = 18.12$ eV and softness was found to be $\zeta = 1/2\eta = 0.38$ eV.

MEPS is used to examine the interaction of a molecular system with its environment, biological recognition studies, the reactivity of chemical systems in nucleophilic and electrophilic reactions, and the study of hydrogen bond interactions. Also MEPS is an isoelectronic density surface mapping method, is a visualization method used to understand the surface and relative polarization [46]. The charges of the structure from negative to positive are defined from red to blue. In Fig. 16, the **Ci** is completely dominated by shades of blue originating from the nitrogen atoms in the main structure**. Ci** was docked with pepsin, trypsin, and DNA to define the interplay against the targets via Auto Dock software. Then, DS 3.5 was used to view the binding affinity of the respective compound to each active surface of the targets. The docking results were interpreted according to binding energy, types of non-bonding interaction and also the conformation of the **Ci** in active area of each target.

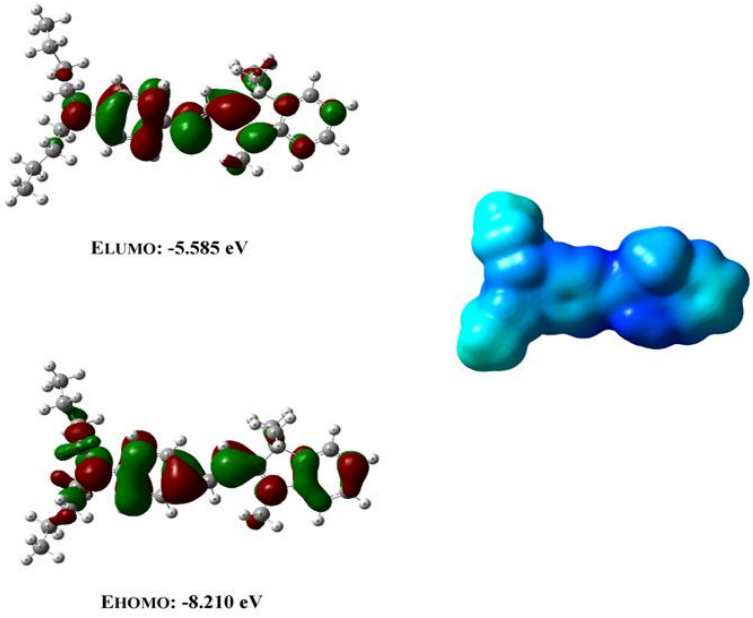


Fig. 14 The HOMO and LUMO molecular orbitals and MEPS map (right side) of **Ci** computed at DFT/B3LYP/6-31+G (d,p) basis set in G09.

Considering its interactions with the targets, **Ci** created two weak carbon H-bonds with Glu13, and Gly217, and nine hydrophobic interactions with the amino acids Ala115, Leu112, Ile120, Tyr75, Phe111 and Ile30 residues of pepsin target in Fig. 10 (top-left side). As a result of the interaction of the second order target, trypsin with **Ci**, the related compound exhibits similar H-bonds and hydrophobic interactions with Ser195, Phe41, Tyr151, Ile73, Tyr39 and His40 residues in binding site of the current target protein, respectively in Fig. 15 (top-right side). Then, the same compound reacted with DNA in the docking study, **Ci** forms electrostatic (A:DG10), weak carbon H-bond (A:DC9, A:DG10, and A:DC11), and hydrophobic interaction (B:DA18), Fig. 15 (bottom left and right side). Docking analysis and details are shown at Table S1.

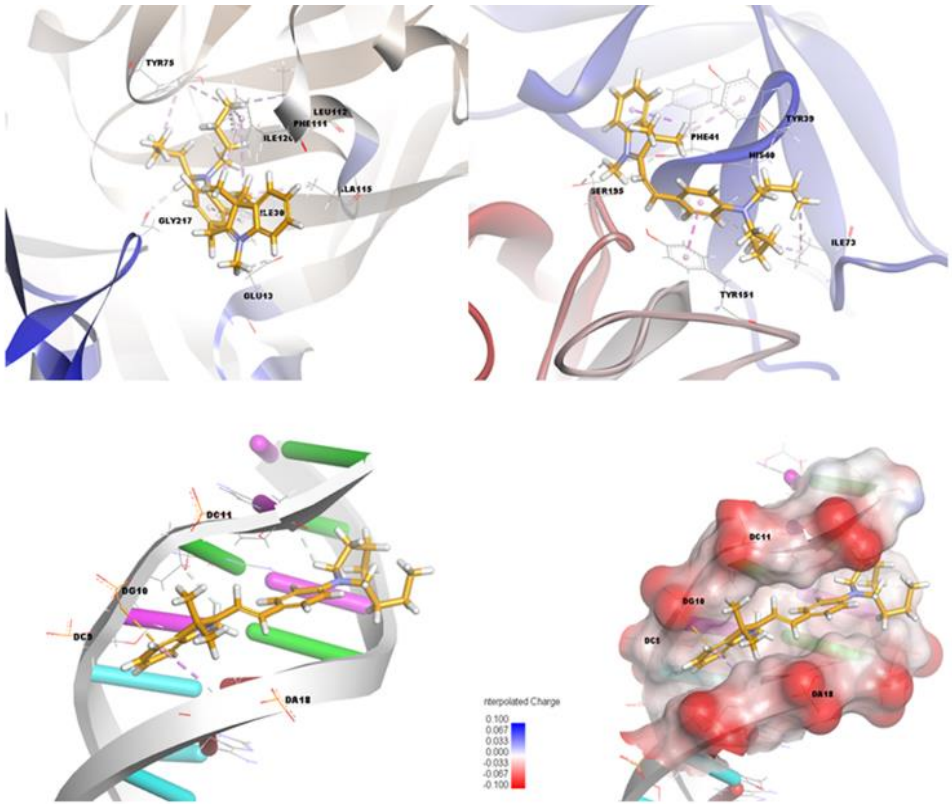


Fig. 15 3D view of docking interactions of **Ci** (orange, stick form), in the binding site of pepsin (top-left side), trypsin (top-right side) and DNA (bottom left and right side).

The docking results displayed that the **Ci** had the best affinity, inhibition constant and RMSD values for pepsin (-7.50 kcal/mol, 114.93 nM and 0.0002). Subsequently, the same compound showed the second and third best binding affinity (-6.90 and -6.80 kcal/mol, 399.21 and 13979 nM and 0.0940 and 0.4260) with trypsin and DNA targets, The results are given in Table S2.

Conclusion

In this study, the **Ci** which is containing indolinium core, have been synthesized and characterized. Its anions selectivity/sensitivity and interactions with protease enzymes (pepsin/trypsin) and ctDNA were studied using spectroscopic methods as well as computational calculations. The fluorescence titration assays showed that binding process is static quenching mechanism to form of **Ci**-pepsin/trypsin complexes. ΔH and ΔS parameters indicated that the binding modes in **Ci**-enzyme complex involved predominantly the electrostatic/hydrophobic interactions between dye and pepsin, and also hydrogen bonds/van der Waals forces between dye and trypsin. The absorption studies indicated that **Ci** interacts with ctDNA in a mode of groove binding. Furthermore, biological activity of **Ci** was further confirmed by molecular docking study on ctDNA and pepsin/trypsin which displayed good tendency with experimental data. The **Ci** indicated hypsochromic effect with a decrease in solvent polarity, and it showed highly selective colorimetric and fluorometric sensing behavior for CN^- in organic and aqueous media. The LOD values of CN^- in the

presence of **Ci** were $4.87x10^{-9}$ M and $9.70x10^{-7}$ M in DMSO and DMSO/H_2O binary mixture, respectively. Moreover, the **Ci** as sensor also showed sensitivity to the CN^- in bitter almond.

Acknowledgements The numerical calculations reported were partially performed at TUBITAK ULAKBIM, High Performance and Grid Computing Center (TRUBA resources).

Author Contributions Bensu Doyuran: Investigation, Writing-original draft. Elmas Gökoğlu: Data curation, Review & Editing. Ayman Zouitini: Synthesis, Investigation, Characterization. Ergin Keleş: Synthesis, Investigation, Characterization. Tugba Taskin-Tok: The theoretical calculations. Nurgül Seferoğlu: The theoretical calculations. Zeynel Seferoğlu: Data curation, Writing-original draft.

Data Availabilitiy All data generated or analysed during this study are included in this published article.

Declarations

Ethics Approval Not applicable

Consent to Participate Not applicable

Consent for Publication Not applicable

Conflicts of interest The authors declare that they have no competing interests

Funding This study was partially supported by Hacettepe University Scientific Research Fund (Project number: FBA2017-12854)

References

1. Li Y, Wei F, Lu Y, He S, Zhao L, Zeng X (2013) Novel mercury sensor based on water soluble styrylindolium dye. Dyes Pigm 96:424-429.
2. Gu J, Rao U, Fabio A, Monte L, Kramer T, Heyny von Haußen R, Hölzer J, V. Goetschy-Meyer J, Mall G, Hilger I, Czech C, Schmidt B (2012) 2-Styrylindolium based fluorescent probes visualize neurofibrillary tangles in Alzheimer's disease. Bioorg Med Chem Lett 22:7667-7671.
3. Metsov S, Simov D, Stoyanov S, Nikolov P (1990) Photophysical characteristics of some 2-styrylindolium dyes. Dyes Pigm. 13:11-19.
4. Promchat A, Rashatasakhon P, Sukwattanasinitt M (2017) A novel indolium salt as a highly sensitive and selective fluorescent sensor for cyanide detection in water. J Hazard Mater 329:255-261.
5. Wang S, Feia X, Guoa J, Yanga Q, Lia Y, Song Y (2016) A novel reaction-based colorimetric and ratiometric fluorescent sensor for cyanide anion with a large emission shift and high selectivity. Talanta 148:229-236.
6. Shiraishi Y, Itoh M, Hirai T (2011) Colorimetric response of spiropyran derivative for anions in aqueous or organic media. Tetrahedron 67:891-897.

7. Perry A, Miles D (2016) An off-the-shelf sensor for colourimetric detection of sulfide. Tetrahedron Lett 57:5788-5793.
8. Liu J, Sun YQ, Huo Y, Zhang H, Wang L, Zhang P, Song D, Shi Y, Guo W (2014) Simultaneous fluorescence sensing of Cys and GSH from different emission channels. J Am Chem Soc 136:574-577.
9. Wu WL, Ma HL, Huang MF, Miao JY, Zhao BX (2017) Mitochondria-targeted ratiometric fluorescent probe based on FRET for bisulfite, Sens Actuators B 241:239-244
10. Yu Q, Zhang KY, Liang H, Zhao Q, Yang T, Liu S, Zhang C, Shi Z, Xu W, Huang W (2015) Dual-emissive nanohybrid for ratiometric luminescence and lifetime imaging of intracellular hydrogen sulfide. ACS Appl Mater Interfaces 7:5462-5470.
11. Gupta SP, Gupta SD (2020) Cancer-leading proteases structures, functions, and inhibition. Elsevier, Chapter 1, India.
12. Pinto MR, Schanze KS (2004) Amplified fluorescence sensing of protease activity with conjugated polyelectrolytes. Proc Natl Acad Sci 101:7505-7510.
13. Li X, Ni T (2016) Binding of glutathione and melatonin to pepsin occurs via different binding mechanisms. Eur Biophys J 45:165-174.
14. Song W, Yu Z, Hu X, Liu R (2015) Dissection of the binding of hydrogen peroxide to trypsin using spectroscopic methods and molecular modeling. Spectrochim Acta Part A 137:286-293.
15. Botti V, Cesaretti A, Ban Z, Crnolatac I, Consiglio G, Elisei F, Piantanida I (2019) Fine structural tuning of styryl-based dyes for f luorescence and CD-based sensing of various ds-DNA/RNA sequences. Org Biomol Chem 17:8243-8258.
16. Barman S, Das J, Biswas S, Maiti TK, Singh NP (2017) A spiropyran-coumarin platform: An environment sensitive photoresponsive drug delivery system for efficient cancer therapy. J Mater Chem B 5:3940-3944.
17. Lakowicz JR (2006) Principles of Fluorescence Spectroscopy, New York, Plenum.
18. a) Becke AD (1993) Density-functional thermochemistry. III. The role of exact exchange. J Chem Phys 98:5648-5651. b) Miehlich B, Savin A, Stoll H, Preuss H (1989) Results obtained with the correlation energy density functionals of becke and Lee, Yang and Parr. Chem Phys Lett 157:200-206. c) Lee C, Yang W, Parr RG (1988) Development of the Colle-Salvetti correlation-energy formula into a functional of the electron density. Phys Rev B 37:785-789.
19. Frisch MJ, et al. (2009) Gaussian 09, Revision A.02. Gaussian, Inc. Wallingford, CT.
20. Cossi M, Barone V (2001) Time-dependent density functional theory for molecules in liquid solutions. J. Chem Phys 115:4708-4717.
21. Bauernschmitt R, Ahlrichs R (1996) Treatment of electronic excitations within the adiabatic approximation of time dependent density functional theory. Chem Phys Lett 256:454-64.
22. Rose Y, Duarte JM, Lowe R, et al. (2021) RCSB protein data bank: architectural advances towards integrated searching and efficient access to macromolecular structure data from the PDB archive. J Mol Biol 433:166704.
23. Accelrys Software Inc. Discovery Studio Modeling Environment, Release 3.5 Accelrys Software Inc (2013) San Diego.

24. Morris GM, Huey R, Lindstrom W, Sanner MF, Belew RK, Goodsell DS, Olson AJ (2009) AutoDock4 and AutoDockTools4: Automated docking with selective receptor flexibility. J Comput Chem 30:2785-2791.
25. Nural Y, Karasu E, Keleş E, et al. (2022) Synthesis of novel acylthioureas bearing naphthoquinone moiety as dual sensor for high-performance naked-eye colorimetric and fluorescence detection of CN^- and F^- ions and its application in water and food samples. Dyes Pigm 198:110006.
26. Park JH, Manivannan R, Jayasudha P, Son YA (2020) Spontaneous optical response towards cyanide ion in water by a reactive binding site probe. Spectrochim Acta Part A 233:118-190.
27. Sante OMDI (2004) World Health Organization, WWprogramme, WHO Staff, Zdrowia SO, WHO, Guidelines for drinking-water quality, Vol 1.
28. Lakowicz JR, Weber G (1973) Quenching of fluorescence by oxygen. A probe for structural fluctuations in macromolecules. Biochemistry 12:4161-4170.
29. Mohseni-Shahr FS, Moeinpour F, Nosrati M (2018) Spectroscopy and molecular dynamics simulation study on the interaction of sunset yellow food additive with pepsin. Int J Biol Macromol 115:273-280.
30. Bi S, Song D, Tian Y, Zhou X, Liu Z, Zhang H (2005) Molecular spectroscopic study on the interaction of tetracyclines with serum albumins. Spectrochim Acta Part A 61: 629-636.
31. Li X, Geng M (2016) Probing the binding of procyanidin B3 to trypsin and pepsin: A multi-technique approach. Int J Biol Macromol 85:168-178.
32. Ross PD, Subramanian S (1981) Thermodynamics of protein association reactions: Forces contributing to stability. Biochemistry 20:3096-3102.
33. Zeng HJ, Yang D, Hua GZ, Yang R, Qu LB (2016) Studies on the binding of pepsin with three pyrethroid insecticides by multi-spectroscopic approaches and molecular docking. J Mol Recognit 29:476-484.
34. Förster T (1948) Intermolecular energy migration and fluorescence. Ann Physics 2: 55-75.
35. Lian S, Wang G, Zhou L, Yanga D (2013) Fluorescence spectroscopic analysis on interaction of fleroxacin with pepsin. Luminescence 28:967-972.
36. Zhang HM, Zhou QH, Wang YQ (2010) Studies on the interactions of 2, 4-dinitrophenol and 2, 4-dichlorphenol with trypsin. J Fluoresc 20:507-516.
37. Moradi S, Ahmadi P, Karami C, Farhadian N, Balaei F, Ansari M, Shahlaei M (2021) Evaluation of the effects of isoniazid and rifampin on the structure and activity of pepsin enzyme by multi spectroscopy and molecular modeling methods. Spectrochim Acta Part A 253:119523.
38. Zhu S, Bai X, Zhu J, Li W, Wang B (2021) Multi-spectral techniques and molecular docking to investigation of the interaction between ferulic acid and pepsin. Spectrochim Acta Part A 251:119442.
39. Matei I, Hillebrand M (2010) Interaction of kaempferol with human serum albumin: A fluorescence and circular dichroism study. J Pharm Biomed Anal 51:768-773.
40 Li X, Ni T (2016) Probing he binding mechanisms of α-tocopherol to trypsin and pepsin using isothermal titration calorimetry, spectroscopic, and molecular modeling methods. J Biol Phys 42:415-434.

41. Siddigui MF, Khan MS, Husain FM, Bano B (2019) Deciphering the binding of carbendazim (fungicide) with human serum albumin: A multispectroscopic and molecular modelling studies. J Biomol Struct Dyn 37:2230-2241.
42. Wang Q, Zhang SR, Ji X (2014) Investigation of interaction of antibacterial drug sulfamethoxazole with human serum albumin by molecular modeling and multi-spectroscopic method. Spectrochim Acta Part A 124:84-90.
43. Li X, Li P (2016) Study on the interaction of β-carotene and astaxanthin with trypsin and pepsin by spectroscopic techniques. Luminescence 31:782-792.
44. Shahabadi N, Falsafi M, Maghsudi M (2017) DNA-binding study of anticancer drug cytarabine by spectroscopic and molecular docking techniques. Nucleosides, Nucleotides and Nucleic Acids 36:49-65.
45. Soudani S, Kaabi K, Jelsch C, Mi JX, Lefebvre F, Nasr CB (2021) Synthesis, X-ray characterisation, hirshfeld surface and theoretical studies of a novel Cd(II) coordination compound bearing 2,3-pyridinedicarboxylic acid, Research Square.
46. Mary YS, Varghese HT, Panicker CY, Girisha M, Sagar BK, Yathirajan HS, Al-Saadi AA, Alsenoy CV (2015) Vibrational spectra, HOMO, LUMO, NBO, MEP analysis and molecular docking study of 2,2-diphenyl-4-(piperidin-1-yl)butanamide, Spectrochim Acta Part A 150:543-556.

Supplementary Files

This is a list of supplementary files associated with this preprint. Click to download.

- SupplementaryInformationCi.docx